Andrzej Flaga (aflaga@pk.edu.pl)
Renata Kłaput
Agnieszka Kocoń

Institute of Structural Mechanics, Faculty of Civil Engineering, Wind Engineering Laboratory, Cracow University of Technology

Wind tunnel tests of wind pressure distributions for four different tent halls

Badania modelowe rozkładu ciśnienia wiatru czterech różnych hal namiotowych

Abstract

This papers concerns measurements of wind pressure distributions on the roofs and side walls of tent hall models. Four tent halls of different shapes and constructions were investigated in the boundary layer wind tunnel at Cracow University of Technology, Poland. On the basis of these measurements, different schemes of wind pressure coefficient distributions for these structures were determined, including mean and extreme values of the coefficients. The obtained results, their analyses and comparisons are of great importance from a structural design point of view for such types of structures.

Keywords: wind tunnel test, tent halls, wind pressure coefficients

Streszczenie

Praca zawiera wyniki badań rozkładu ciśnienia wiatru na dachach i ścianach bocznych hal namiotowych. W tunelu aerodynamicznym Politechniki Krakowskiej przebadano cztery hale namiotowe różnych kształtów. Na podstawie tych pomiarów określono schematy rozkładów współczynników ciśnienia wiatru oraz średnie i ekstremalne wartości współczynników. Otrzymane wyniki oraz ich analizy i porównania mają duże znaczenie z punktu widzenia projektowania tego typu konstrukcji.

Słowa kluczowe: tunel aerodynamiczny, hale namiotowe, współczynniki ciśnienia wiatru

1. Introduction

The wind action on four tent halls of various roof shapes and constructions was determined from wind tunnel experiments conducted in the boundary layer wind tunnel at Cracow University of Technology. Investigations concerned the variables of wind angle, terrain roughness and roof shape.

Tent halls are made of aluminium profiles covered with a two-sided textile membrane enhanced with PCV layers. These kinds of structures are widely used in low-rise industrial buildings, sport facilities, warehouses. However, their relatively light weight and flexibility make them vulnerable to wind action; therefore, knowledge of wind pressure distribution on the side walls and roofs is essential in the structural design of these objects.

Many researchers have investigated the problem of wind action on objects of different shapes [3, 4, 8]. On the basis of these investigations, it was concluded that the geometry of a structure has an influence on pressure distribution on the building walls. The local wind pressures on walls of different low-rise buildings have been investigated by, inter alia, Gavanski & Uematsu [2], Alrawashdeh & Stathopoulos, 2015 [2]. In the case of light structures, peak local wind pressures are the most important in terms of object safety – this was considered in Pratt & Kopp [6] and Saathoff & Melbourne [7].

The main goal of this paper is to present the results of wind tunnel tests on four different types of tent halls. For each hall model, wind pressures were measured on the external surfaces of the roofs and side walls of the tent halls. On the basis of wind pressure at the measurement points and the reference pressure, the mean and extreme wind pressure coefficients were calculated. The obtained values of aerodynamic coefficients can be used in static-strength calculations of major structural elements.

2. Description of tent halls models

The models used in the wind tunnel tests were made at the following scales: 1:37.5 – model A; 1:62.5 – model B; 1:71.4 – model C; 1:16 – model D. The scales were chosen in such a way as to obtain models within a similar range of dimensions? The elements of the A-C models were made from extruded polystyrene XPS plates and the D model was made from laminated Plexiglas which had been cut by a laser. Each model consists of side walls, a roof and a base. Figure 1 presents the schematics of the tent halls models.
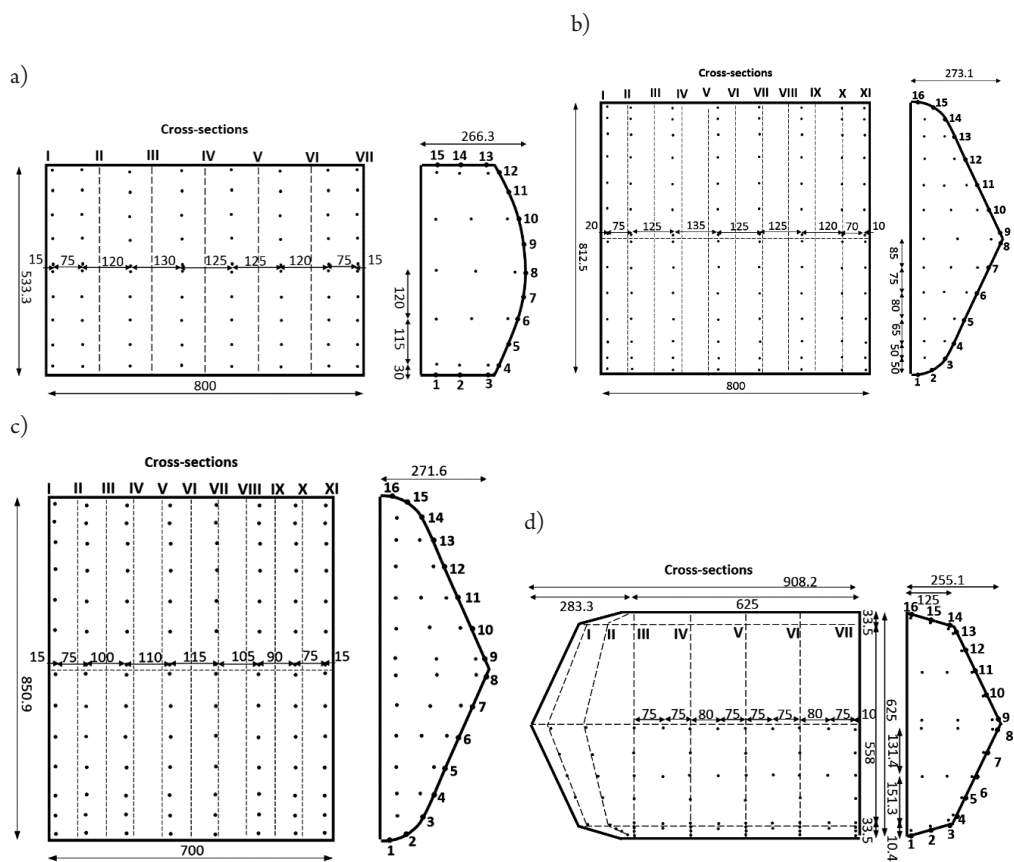
Fig. 1. Schematics of the tent halls models investigated in the wind tunnel tests: a) model A, b) model B, c) model C, d) model D

3. Description of the research

3.1. Simulation of boundary layer

The presented tests were conducted in the boundary layer wind tunnel a the Wind Engineering Laboratory at Cracow University of Technology. The basic dimensions of the working section of the wind tunnel are: 2.20 m (width), 1.40 m (height), 10.00 m (length). In the initial part of the investigations, the structure of the wind flow was determined. The wind profile was formed with the use of a barrier with a height of 20 cm. Thermo-anemometers were used to measure the mean and fluctuation of the wind velocity at 6 points located in the working section of the wind tunnel at heights from 5 cm to 30 cm above the floor level. Using power-low form of wind profile and data obtained from measurements, the following wind profile parameters were obtained:

$$V(z) = V_{ref} \left(\frac{z}{z_{ref}} \right)^{\alpha}$$

$$z_{ref} = 0.3 \text{ m}, \ V_{ref} = 14.7 \frac{\text{m}}{\text{s}}, \ \alpha = 0.18.$$

where:

z_{ref} – reference height $[\text{m}]$,

α – exponent depend on terrain roughness,

V_{ref} – reference wind velocity.

The obtained wind profile and turbulence intensity profile are shown in Fig. 2 a) and b). The red points mark values from wind tunnel tests and the black line marks function determined by least-square regression. The turbulence intensity I_v [%] on the reference level $(z_{ref} = 0.3 \text{ m})$ was 19%. The power spectral density (Fig. 2c) was made from the velocity generated with time intervals of 0.002 s over 20 s (resulting in 10,000 samples) and compared with the Davenport spectrum.
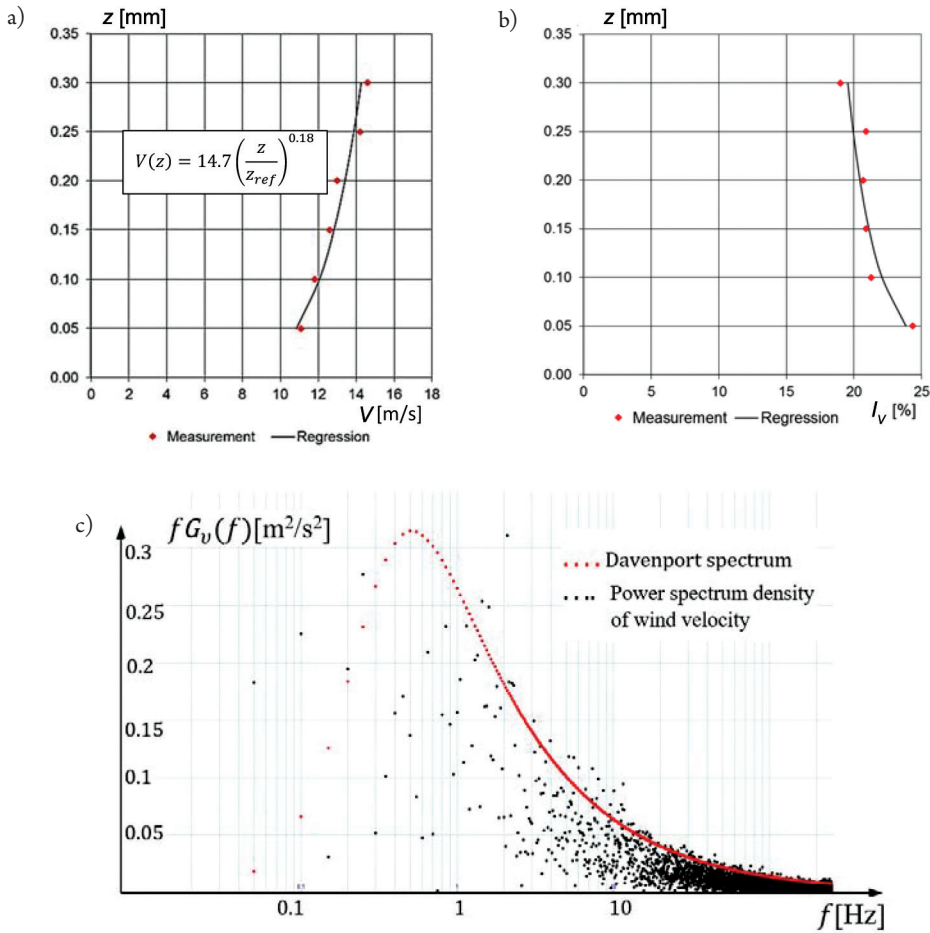

Fig. 2a) vertical profile of mean wind velocity in the wind tunnel; b) turbulence intensity profile; c) power spectrum density of wind velocity for measurement point at reference height and Davenport spectrum determined by least-square regression

3.2. Characteristics of the wind tunnel tests

Models of tent halls were placed in the working section of the wind tunnel on a round turnable table with a diameter of 2 m enabling the change of the angle of wind onflow onto the examined objects. The angle was changed in increments of 45 degrees for different measurement conditions. Figure 3 shows the orientation of the model with respect to the wind directions and Fig. 4 presents the tent halls in the measuring position.

Due to the symmetry of the tested tent halls, the measurement points were distributed only on half of the model. At each of these points, wind velocity pressures as a function of time were measured. The wind velocity reference pressure (q_{ref}) was measured at the reference point as a difference of the total pressure obtained from a Prandl tube and the static pressure obtained from a static pressure probe.

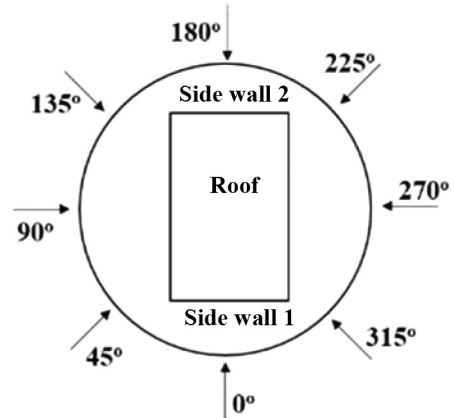

Fig. 3. Orientation of the model with respect to the wind directions
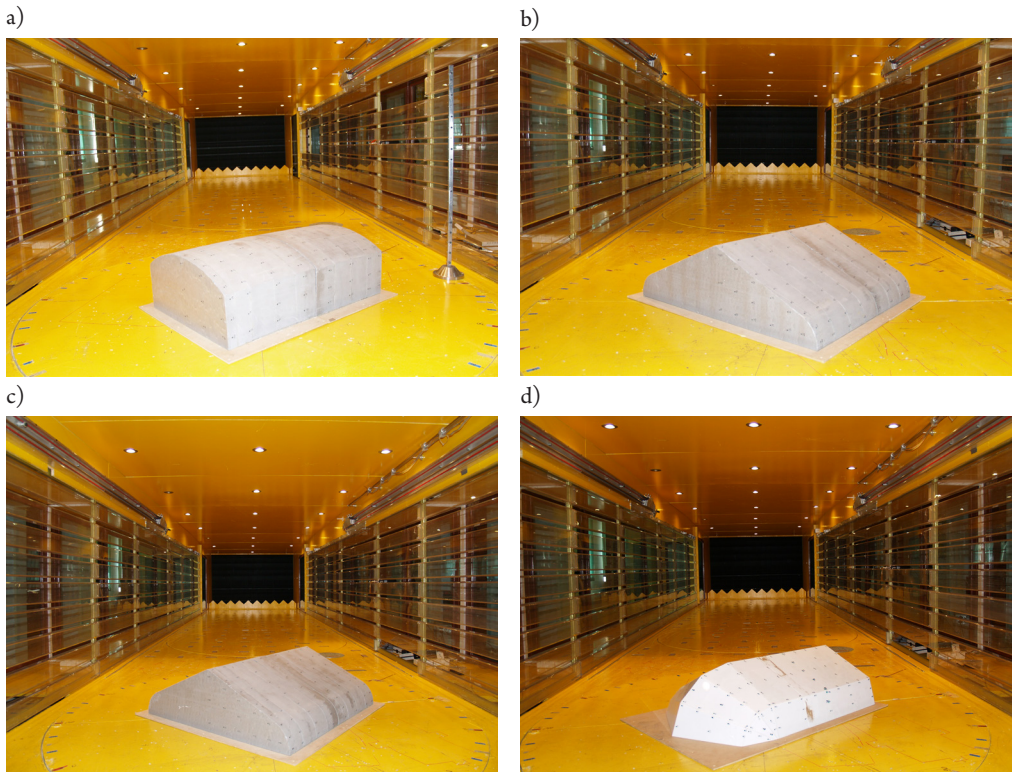
a)
b)
c)
d)

Fig. 4. View of the tent hall models in the working section of the boundary layer wind tunnel:
a) model A, b) model B, c) model C, d) model D

The measurements were performed using the tent hall models equipped with pressure sensors distributed at various heights above the ground on the outer walls of the models. The sensors have been connected to the pressure scanners making possible simultaneously collection of instantaneous wind pressure time series. The scan rate of each series was 200 Hz and data was recorded over a period of 30 s. A 64-channel parallel type pressure scanner was used for the measurements.

Measurements at each point were then interpolated to obtain the distribution of wind pressures on the whole roof; thus, the pressure coefficients were determined for different tent hall cross sections.

4. Basic denotations and definitions

The wind pressures were measured on the external surfaces of the roofs and side walls of the models. The mean wind pressure coefficients were calculated according to the formula:

$$C_{pe} = \frac{p_e}{q_{ref}} \tag{1}$$

where:

p_e – mean wind pressure,

q_{ref} – reference pressure of the onflowing air at the model height.

Minimum and maximum local values of wind pressure coefficients were calculated on the basis of wind pressure and the standard deviation of mean wind pressure using the following formulas:

$$C_{pe}^{max,l} = \frac{p_e + g_p^l \cdot p_e^\sigma}{q_{ref}}; \quad C_{pe}^{min,l} = \frac{p_e - g_p^l \cdot p_e^\sigma}{q_{ref}} \tag{2}$$

where:

p_e^σ – standard deviation of instantaneous wind pressure $p_e(t)$;

g_p^l – local peak pressure factor.

Coefficients calculated according formulae (1) and (2) were determined for 8 angles of wind flow in accordance with Fig. 3.

In the structural design of the main bearing structures (frames) of tent halls, the following important questions should be considered:

1. Maximum and minimum local wind pressures never occur simultaneously at different points on the surface of a tent hall. Thus, in the design process of the main bearing structures (frames) of the tent halls, some average values of local wind pressures can be adopted.
2. Tent halls are temporary objects; therefore, using a simplified deterministic approach to calculate the wind action on these engineering objects is justified.
3. Usually, the load-bearing frames of a tent hall are similar in terms of geometry, construction material, solutions of structural nodes, and cross sections of frame columns and transoms.
4. The number of frames and number of air onflow cases for each tent hall requires around 200 calculations for static issues alone, which are related to mean wind action.

The number of calculation significantly increases if combinations of the following main actions on the structure are taken into account: self-weight, live loads, wind action, snow load, thermal actions.

5. Wind action is a random spatial-temporal process. In order to properly calculate such an action, it is necessary to know the spatial-temporal or space-frequency characteristics of these processes which can be obtained, for example, in model tests in wind tunnels, which extremely complicate not only the model tests but also the subsequent processing and analysis of tests results.

Taking all this into account, it is appropriate to use a simplified calculation approach of wind action on tent halls based on the quasi-static deterministic model proposed in this paper. This is characterised by the following assumptions:

1. The basis for determining the deterministic quasi-static actions is formula (1) and formula (2) in which the local peak pressure factor g_p^l related to the bearing structures (frames) of the investigated tent halls is of the order of 1. Thus, the following formulae were used in further considerations:

$$C_{pe}^{\max,l} = \frac{p_e + p_e^\sigma}{q_{ref}}; \ C_{pe}^{\min,l} = \frac{p_e - p_e^\sigma}{q_{ref}} \tag{3}$$

2. The maximum and minimum values from all coefficients – $C_{pe}^{\max,l}$ and – $C_{pe}^{\min,l}$ are determined for each wind direction and for a given frame – these are denoted as: $C_{pe}^{\max}$ i $C_{pe}^{\min}$.

3. A similar procedure can be used for the average values of the coefficient C_{pe} determining the maximum and minimum values for each wind direction and for a given frame: $C_{pe,\max}$ and $C_{pe,\min}$.

4. The differences of the extreme coefficients are then determined, i.e.:

$$\left(C_{pe}^{\max} - C_{pe,\max}\right) \text{ and } \left(C_{pe}^{\min} - C_{pe,\min}\right) \tag{4}$$

These coefficients are schematically presented in Fig. 5.

5. The above quantities are the basis for determining the equivalent surface action for a given frame from according to the formulas:

$$p_{eq}^{\max} = \left(C_{pe} + C_{pe}^{\max} - C_{pe,\max}\right)q_{ref} \tag{5}$$

$$p_{eq}^{\min} = \left(C_{pe} + C_{pe}^{\min} - C_{pe,\min}\right)q_{ref} \tag{6}$$

6. Equivalent, maximal and minimal wind action for a given frame and for a given wind direction, per unit length of the frame column or transom, are determined by the formulas:

$$w_{eq}^{\max} = p_{eq}^{\max} L\gamma \tag{7}$$

$$w_{eq}^{\min} = p_{eq}^{\min} L\gamma \tag{8}$$

where: L – distance between adjacent span frames or half of the distance between the outer frame and the adjacent frame; γ – wind action coefficient (partial safety coefficient), which is proposed to be adopted at the level of 1.5, due to the adopted, simplified deterministic model of wind action on the tent halls. This coefficient according to Eurocode PN/EN 1991-1-4, is usually assumed at a level of 1.3 for typical buildings.

Taking into account the above remarks, coefficients: C_{pe}, C_{pe}^{max}, $C_{pe\,max}$, C_{pe}^{min}, $C_{pe\,min}$ were considered in the further data processing and analysis of tests results.

Fig. 5. Schematic presentation of respective extreme coefficients

5. Results of the wind tunnel tests

The results in Figs. 6–9 present distributions of mean wind pressure coefficients on the external surfaces of all the tent hall models. Because of the symmetry of the model, only results at 3 angles of wind attack (0°, 45°, 90°) for the A, B and C models, and at 5 angles of

Fig. 6a) contour map of C_{pe} distributions on external surfaces; b) mean wind pressure coefficient for all cross sections of tent hall model 'A' at wind directions 0°, 45°, 90°

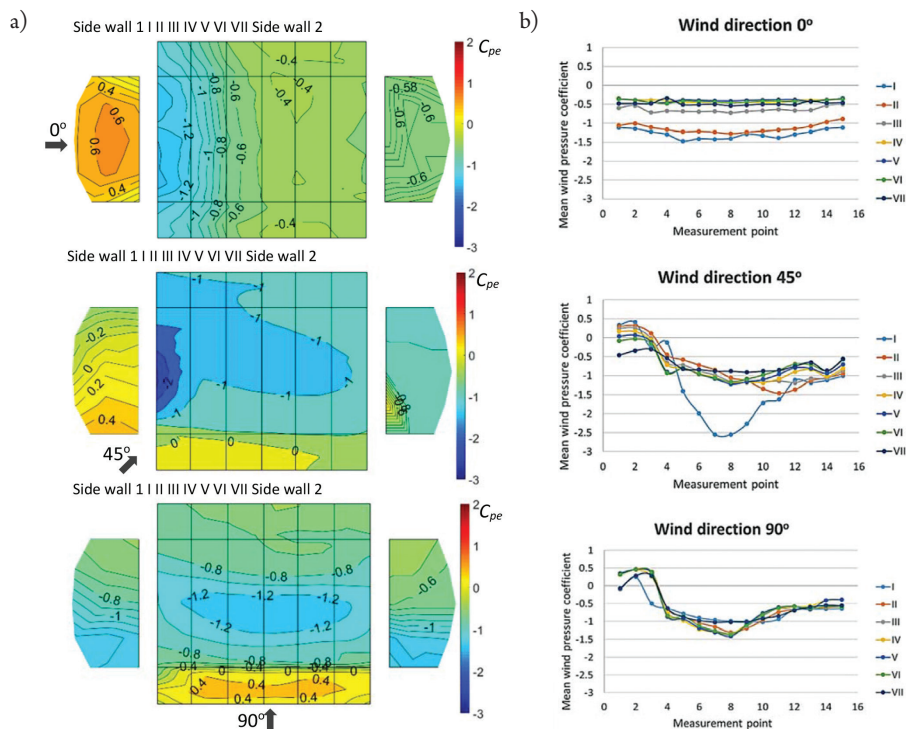wind attack (0°, 45°, 90°, 135°, 180°) for the D model have been illustrated and subsequently analysed. Furthermore, the extreme values of the mean wind pressure coefficients (C_{pe}) and the peak wind pressure coefficients (C_{pe}^{max}, C_{pe}^{min}) for both of the side walls, the edge cross sections and the middle cross sections are summarised in Tables 1–4.

Table 1. The extreme values of the mean wind pressure coefficients C_{pe} and peak wind pressure coefficients C_{pe}^{max}, C_{pe}^{min}, on the side walls, edge cross section and middle cross section of model 'A'

Angle [°]	Cross section I (edge)				Cross section IV (middle)			
	C_{pe}		C_{pe}^{max}	C_{pe}^{min}	C_{pe}		C_{pe}^{max}	C_{pe}^{min}
	max	min			max	min		
0	−1.1	−1.5	−0.2	−2.3	−0.4	−0.5	−0.1	−0.7
45	0.4	−2.5	0.8	−2.6	0.2	−1.2	0.4	−1.3
90	0.3	−1.0	0.6	−1.6	0.5	−1.4	0.7	−1.5

Angle [°]	Side wall 1				Side wall 2			
	C_{pe}		C_{pe}^{max}	C_{pe}^{min}	C_{pe}		C_{pe}^{max}	C_{pe}^{min}
	max	min			max	min		
0	0.7	0	1.0	−0.2	−0.6	−0.6	−0.5	−0.8
45	0.5	−0.5	0.8	−0.6	−0.8	−1.0	−0.7	−1.1
90	−0.5	−1.4	−0.3	−1.8	−0.5	−1.4	−0.2	−1.6

Fig. 7a) contour map of C_{pe} distributions on external surfaces; b) mean wind pressure coefficient for all cross sections of tent hall model 'B' at wind directions of 0°, 45°, 90°

Table 2. The extreme values of the mean wind pressure coefficients C_{pe} and peak wind pressure coefficients C_{pe}^{max}, C_{pe}^{min}, on the side walls, edge cross section and middle cross section of model 'B'

Angle [°]	Cross section I (edge)				Cross section VI (middle)			
	C_{pe}		C_{pe}^{max}	C_{pe}^{min}	C_{pe}		C_{pe}^{max}	C_{pe}^{min}
	max	min			max	min		
0	−1.1	−1.6	−0.4	−2.1	−0.3	−0.5	−0.2	−0.6
45	0.1	−3.0	0.6	−3.2	0.1	−1.8	0.2	−1.9
90	0	−0.9	0.3	−1.2	0.4	−1.1	0.6	−1.2

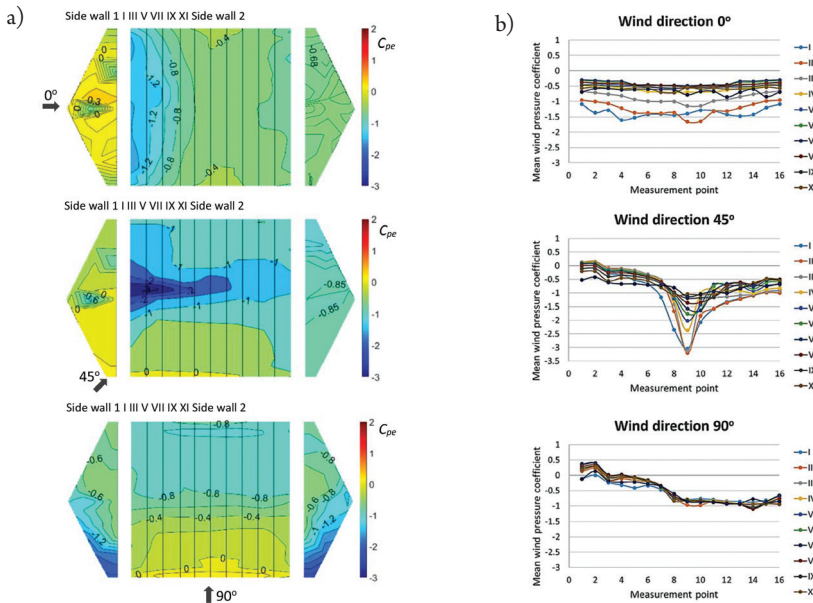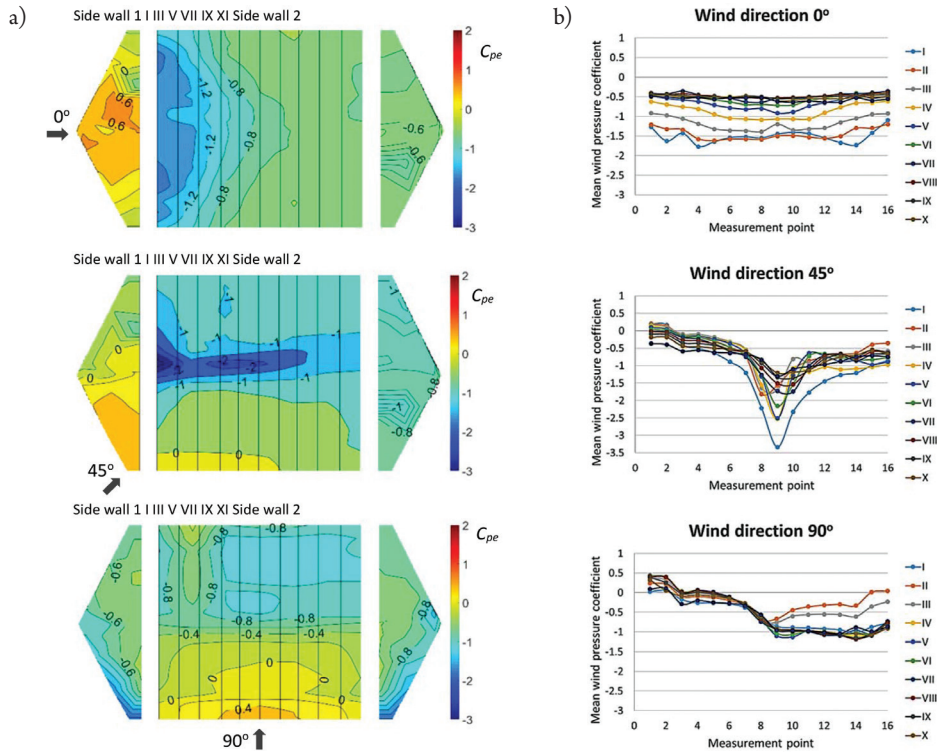| Angle [°]	Side wall 1				Side wall 2			
	C_{pe}		C_{pe}^{max}	C_{pe}^{min}	C_{pe}		C_{pe}^{max}	C_{pe}^{min}
	max	min			max	min		
0	0.4	−0.7	0.9	−0.7	−0.6	−0.7	−0.4	−0.7
45	0.3	−1.1	1.1	−1.1	−0.8	−1.1	−0.6	−1.1
90	−0.4	−2.1	0.2	−2.1	−0.5	−2.4	−0.1	−2.4

Fig. 8a) contour map of C_{pe} distributions on external surfaces; b) mean wind pressure coefficient for all cross sections of tent hall model 'C' at wind directions of 0°, 45°, 90°

Table 3. The extreme values of the mean wind pressure coefficients C_{pe} and peak wind pressure coefficients C_{pe}^{max}, C_{pe}^{min}, on the side walls, edge cross section and middle cross section of model 'C'

Angle [°]	Cross section I (edge)				Cross section VI (middle)			
	C_{pe}		C_{pe}^{max}	C_{pe}^{min}	C_{pe}		C_{pe}^{max}	C_{pe}^{min}
	max	min			max	min		
0	−1.1	−1.8	−0.7	−3.6	−0.4	−0.7	−0.2	−1.1
45	0.2	−3.3	0.6	−3.6	0	−2.2	0.2	−2.5
90	0.1	−1.0	1.3	−1.7	0.4	−1.1	0.6	−1.2

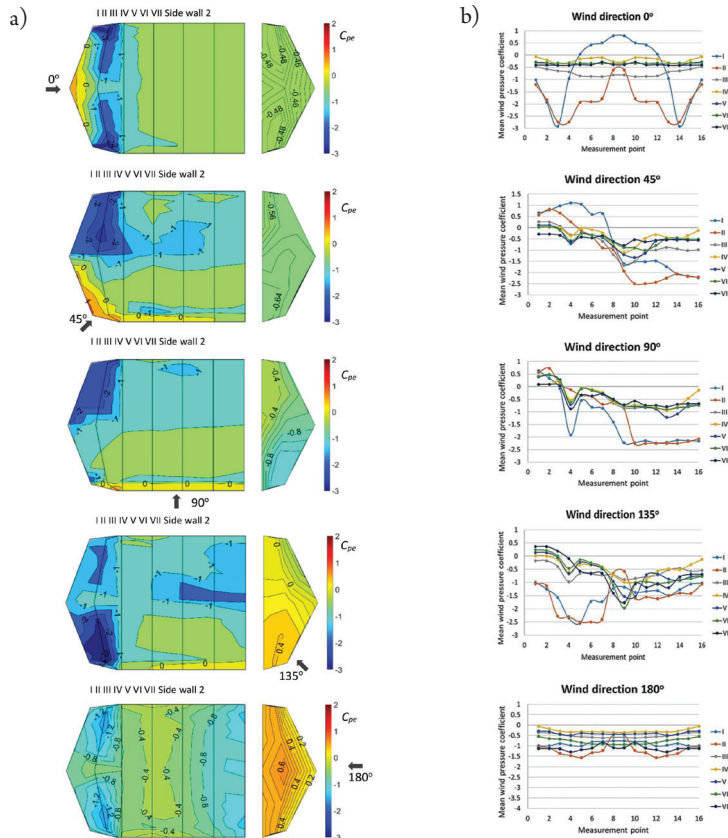| Angle [°]	Side wall 1				Side wall 2			
	C_{pe}		C_{pe}^{max}	C_{pe}^{min}	C_{pe}		C_{pe}^{max}	C_{pe}^{min}
	max	min			max	min		
0	0.7	−0.2	1.1	−0.6	−0.4	−0.8	−0.4	−0.9
45	0.5	−0.4	0.8	−1.0	−0.6	−1.0	−0.6	−1.3
90	−0.3	−1.9	0	−2.6	−0.3	−1.8	−0.1	−2.5

Fig. 9a) contour map of C_{pe} distributions on external surfaces; b) mean wind pressure coefficient for all cross sections of tent hall model 'D' at wind directions of 0°, 45°, 90°

Table 4. The extreme values of the mean wind pressure coefficients C_{ep} and peak wind pressure coefficients C_{pe}^{max}, C_{pe}^{min} on the side walls, edge cross section and middle cross section of model 'D'

Angle [°]	Cross section III (edge)				Cross section V (middle)			
	C_{pe}		C_{pe}^{max}	C_{pe}^{min}	C_{pe}		C_{pe}^{max}	C_{pe}^{min}
	max	min			max	min		
0	−0.5	−0.9	−0.4	−1.0	−0.3	−0.4	−0.2	−0.5
45	0.3	−1.7	0.4	−2.0	0.1	−1.3	0.3	−1.6
90	0.5	−0.9	0.7	−1.1	0.5	−1.2	0.7	−1.5
135	−0.2	−1.0	−0.1	−1.3	0.1	−1.5	0.3	−2.0
180	−0.4	−0.6	−0.3	−0.8	−0.3	−0.5	−0.1	−0.8

Angle [°]	Side wall 1 (cross section I, II)				Side wall 2			
	C_{pe}		C_{pe}^{max}	C_{pe}^{min}	C_{pe}		C_{pe}^{max}	C_{pe}^{min}
	max	min			max	min		
0	0.8	−2.9	1.4	−3.0	−0.4	−0.5	−0.4	−0.6
45	1.1	−2.5	1.6	−2.7	−0.5	−0.7	−0.4	−0.8
90	0.7	−2.2	1.3	−2.4	−0.3	−1.1	−0.1	−1.6
135	−0.6	−2.5	−0.3	−2.7	0.4	−0.4	0.6	−0.5
180	−0.5	−1.6	−0.3	−1.9	0.6	0.2	0.9	−0.1

In the case of the A model, the following conclusions can be drawn from the measurement analysis: the highest negative pressure appears in the half part of all the cross sections. The highest value of the C_{pe}^{min} coefficient is −2.6 – this occurred in the middle part of the roof with a wind direction of 45° in the first cross section. The highest value of the C_{pe}^{max} coefficient is 1.0 – this occurred on side wall I with a wind direction of 0°. The highest wind action occurred at the wind attack angle of 45° for edge the cross section and 90° for middle cross section.

In the case of the B model, the highest value of the C_{pe}^{min} coefficient is −3.2 – this occurred at the top of the roof and with a wind direction of 45° in the first cross-section of tent hall. The highest value of the C_{pe}^{max} coefficient is 1.1 – this occurred on side wall I with a wind direction of 45°. The highest wind action occurred with wind attack angles of 45° for both the edge cross section and the middle cross section.

The shape of tent hall C is similar to that of the previous hall (B), they differ only in the length with hall B being longer than hall C. The difference for both objects is negligible. The highest value of the C_{pe}^{min} coefficient is −3.6 – this occurred at the top of the roof with a wind direction of 45° and in the first cross section of the tent hall. The highest value of the C_{pe}^{max} coefficient is 1.3 – this occurred on the side wall with a wind direction of 90° and in the first cross section of the tent hall.

On the basis of C_{pe}^{min} the measurement results obtained for tent hall D, the following conclusions can be formulated: the highest value of coefficient is −3.0 – this occurred at a wind direction of 0° in the first cross section of the tent hall. The highest value of the C_{pe}^{max} coefficient is 1.6 – this occurred at a wind direction of 45° and in the first cross section of tent hall D.

Peak wind pressure coefficients C_{pe}^{max}, C_{pe}^{min} on the external surfaces for all tent halls are presented in Table 5.

Table 5. Peak wind pressure coefficients C_{pe}^{max}, C_{pe}^{min} on the external surfaces of the tent halls

Tent hall		A		B		C		D	
Wind direction	Surface	C_{pe}^{max}	C_{pe}^{min}	C_{pe}^{max}	C_{pe}^{min}	C_{pe}^{max}	C_{pe}^{min}	C_{pe}^{max}	C_{pe}^{min}
0°	side wall 1	1.0	−0.2	0.9	−0.7	1.1	−0.6	1.4	−3.0
	roof	0.5	−2.3	0.2	−2.2	−0.1	−2.1	0	−1.0
	side wall 2	−0.5	−0.8	−0.4	−0.7	−0.4	−0.9	−0.4	−0.6
45°	side wall 1	0.8	−0.6	1.1	−1.1	0.8	−1.0	1.6	−2.7
	roof	0.8	−2.6	0.6	−3.3	0.6	−3.1	0.4	−2.0
	side wall 2	−0.7	−1.1	−0.6	−1.1	−0.6	−1.3	−0.4	−0.8
90°	side wall 1	−0.3	−1.8	0.2	−2.1	0	−2.6	1.3	−2.4
	roof	0.8	−1.6	0.6	−1.6	1.3	−1.8	0.7	−1.5
	side wall 2	−0.2	−1.6	−0.1	−2.4	−0.1	−2.5	−0.1	−1.6

Figure 10 presents a comparison of the measured extreme values of the peak wind pressure coefficients C_{pe}^{max}, C_{pe}^{min} on the side walls and roof of all of the tent halls. For the wind direction perpendicular to the side wall (0°), the pressure distribution on the analysed roofs slightly depends on the shape of the tent hall. In the edge cross section accrues the lowest value of the mean pressure wind pressure coefficients up to −1.8 for the C tent hall.
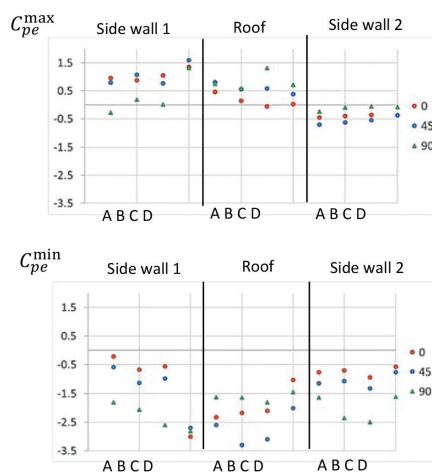

Fig. 10. Distribution of the extremal value of C_{pe}^{max}, C_{pe}^{min} coefficients on the side walls and roof of tent hall models A, B, C, D

Maximum negative wind pressure appears in the edge cross section for all of the analysed halls. For the A, B, and C tent halls, the maximum negative pressure occurs in the middle of the cross section. Tent hall D presents slightly different results because the highest negative pressure can be observed in the lower part of the wall.

The mean external wind pressure coefficient has extreme values in the case of hall A for angles of wind onflow of 90° for the middle cross section and 45° for the edge cross sections. During the analysis of the results, differences appearing for C_{pe} for B and C can also be observed. These halls have similar geometry – they differ only in the length with hall B being longer than hall C. The negative pressure for C is higher than for B and this trend is visible in results for all of the cross sections. It can be concluded that the length of the hall has an influence on the mean external wind pressure coefficient – the smaller the length, the higher the value of C_{pe}.

To summarise, in most of the analysed cases, the extremal mean wind pressure coefficient appears in the middle part of the edge cross section of tent halls. The shape of the hall cross section has a significant influence on the value of this coefficient. The highest values of C_{pe} appears for the 45° angle of wind onflow; therefore, it is essential to take into consideration this information in the design of such structures.

6. Conclusions

The measurements of wind pressure distributions on the surfaces of tent halls of different shapes allow the following conclusions to be drawn:

- ▸ The shape of the tent hall has a significant influence on the wind action on the analysed surfaces.
- ▸ The highest values of negative wind pressure appear on the roof edge, especially in the edge cross section for an angle of wind attack of 45°. Sharp roof edges generate higher values of wind pressure coefficients.
- ▸ The highest values of positive wind pressure occur on the longitudinal side walls for wind onflowing at an angle of 90°.

References

[1] Alrawashdeh H., Stathopoulos T., *Wind pressures on large roofs of low buildings and wind codes and standards, J. Wind Eng. Ind. Aerodyn.* 147, 2015, 212–225.
[2] Gavanski E., Uematsu Y., *Local wind pressures acting on walls of low-rise buildings and comparisons to the Japanese and US wind loading* provisions, J. Wind Eng. Ind. Aerodyn., 132, 2014, 77–91.
[3] Hoxey R.P., Moran P., *A full-scale study of the geometric parameters that influence wind loads on low-rise buildings*, J. Wind Eng. Ind. Aerodyn., 13 (1–3), 1983, 277–288.

[4] Kim K.C., Ji H.S., Seong S.H., *Flow structure around a 3-D rectangular prism in a turbulent boundary layer*, J. Wind Eng. Ind. Aerodyn., 91, 2003, 653–669.

[5] PN-EN 1991-1-4: Action on structures. Part 1–4: General action (in Polish).

[6] Pratt F.N., Kopp G.A., *Velocity field measurements above the roof of a low-rise building during peak suctions*, J. Wind Eng. Ind. Aerodyn., 133, 2014, 234–241.

[7] Saathoff P.J., Melbourne W.H., *Effects of free-stream turbulence on surface pressure fluctuations in a separation bubble*, J. Fluid Mech., 337, 1997, 1–24.

[8] Stathopoulos T., *Wind loads on low-rise buildings – A review of the state of the art*, Eng. Struct., 6, 1984, 119–135.

[9] Tielman H.W., *Wind tunnel simulation of wind loading on low-rise structures: a review*, J. Wind Eng. Ind. Aerodyn., 91, 2003, 1627–1649.